Synthesis of Amine-Cured, Epoxy-Layered Silicate Nanocomposites: The Influence of the Silicate Surface Modification on the Properties

Xavier Kornmann,[1] Ralph Thomann,[2] Rolf Mülhaupt,[2] Jürgen Finter,[3] Lars Berglund[1]

[1]*Division of Polymer Engineering, Luleå University of Technology, S-97187 Luleå, Sweden*
[2]*Freiburg Materials Research Centre and Institute for Macromolecular Chemistry, Albert-Ludwigs-Universität, Stefan-Meier-Straße 21, D-79104 Freiburg im Breisgau, Germany*
[3]*Vantico AG, Postfach K-401.P.08, CH-4002 Basel, Switzerland*

Received 8 February 2002; accepted 20 March 2002

ABSTRACT: Fluorohectorites were rendered organophilic through the cation exchange of sodium intergallery cations for protonated monoamine, diamine, and triamine oligopropyleneoxides and octadecylamine, benzylamine, and adducts of octadecylamine and benzylamine with diglycidyl ether of bisphenol A (DGEBA). The influence of the silicate surface modification and compatibility on the morphology and thermal and mechanical properties was examined. Surface modification with protonated octadecylamine and its adduct with DGEBA promoted the formation of microscale domains of silicate layers separated by more than 50 Å, as evidenced by transmission electron microscopy and wide-angle X-ray scattering. Young's modulus of these two nanocomposites increased parabolically with the true silicate content, whereas conventionally filled composites exhibited a linear relationship. The highest fracture toughness was observed for conventionally filled composites. © 2002 Wiley Periodicals, Inc. J Appl Polym Sci 86: 2643–2652, 2002

Key words: nanocomposites; thermosets; structure-property relations

INTRODUCTION

Polymer nanocomposites are stimulating fundamental and applied research because of their unusual physical and chemical properties. Their surprising behavior is related to the presence of nanoscale matrix reinforcements with high aspect ratios. In particular, polymer-layered silicate nanocomposites are attracting interest because of their high performances at very low layered silicate contents. Substantial improvements in the mechanical properties,[1,2] barrier properties,[3,4] and solvent resistance,[5] as well as low flammability,[6,7] are some of the numerous advantages offered by this new class of materials.

The surfaces of nanofillers based on layered silicates are readily modified through the exchange of the intergallery cations situated between the silicate layers. The 2:1 layered silicates consist of two fused silica tetrahedral sheets sandwiching an edge-shared octahedral sheet. Isomorphous substitutions in the tetrahedral and octahedral sheets cause an excess of negative charges within the silicate layers. These negative charges are counterbalanced by cations situated between the silicate layers. These inorganic cations can be exchanged for organophilic cations to obtain organosilicates, which are effectively dispersed in organic media such as polymers. The first surface modifiers used in the synthesis of polymer-layered silicate nanocomposites (polyamide 6/clay hybrids) were amino acids. They were used because they intercalated easily and copolymerized with aminocapronic acid intercalated between the silicate layers.[8,9] Later, alkylammonium ions, which had long been known to lower the surface energy of layered silicates,[10,11] were used in various polymer systems to synthesize nanocomposites. Lan et al.[12] showed that the chain length of alkylammonium ions has a direct influence on the nanostructure of epoxy-layered silicate nanocomposites. Varying the chain length of alkylammonium ions is the key to facilitating the diffusion of diglycidyl ether of bisphenol A (DGEBA) and curing agent molecules between the silicate layers because it reduces the electrostatic interactions present between the silicate layers. This is an important requirement for achieving the separation of the silicate layers and the in situ formation of anisotropic nanoparticles. The major problem concerning the use of alkylammonium ions for the synthesis of epoxy-layered silicate nano-

Correspondence to: X. Kornmann (xavier.kornmann@empa.ch).

Contract grant sponsor: Sonderforschungsbereich SFB 428, Deutsche Forschungsgemeinschaft.
Contract grant sponsor: Fonds der Chemischen Industrie.
Contract grant sponsor: Swedish Engineering Research Council.

composites is their relatively poor compatibility with the polar epoxy matrix. The main objective of this study was to examine different surface modifiers as candidates for the synthesis of epoxy-layered silicate nanocomposites.

In previous articles, we demonstrated that both the nature of the layered silicate[13] and that of the curing agent[14] had a direct influence on the structure and properties of epoxy-layered silicate nanocomposites. In this work, our objective was to show how the nature of the surface modifier influenced the structure and properties of these nanocomposites. Several organosilicates treated with surface modifiers of different polarities were used in the syntheses of the nanocomposites. Their structure was characterized with both wide-angle X-ray scattering (WAXS) and transmission electron microscopy (TEM) measurements. The results showed that the molecular structure of the surface modifier should be optimized to ensure the correct polarity of the silicate surface and promote the diffusion of DGEBA and curing agent molecules between these layers and, therefore, achieve the separation of the silicate layers.

EXPERIMENTAL

Materials

The synthetic layered silicate Somasif ME-100 with a cation exchange capacity (CEC) of 100 mequiv/100 g was used in this study. This fluorohectorite, prepared by the heating of talcum in the presence of Na_2SiF_6 for several hours in an electric furnace at a high temperature, was supplied by CO-OP, Ltd. (Tokyo, Japan). Different surface modifiers were used in this study: octadecylamine (ODA) and benzylamine (BA) from Fluka Chemie GmbH (Deisenhofen, Germany); polyoxyalkylene monoamines, diamines, and triamines (Jeffamines M600, D230, D400, and T403) from Huntsman Corp. (Hamburg, Germany); and adducts based on a low molecular weight DGEBA resin ($n = 0$), Araldite MY790-1, provided by Vantico AG (Basel, Germany). The matrix was a conventional DGEBA resin, Araldite CY 225, provided by Vantico. It was used in combination with the polyoxyalkylene diamine curing agent Jeffamine D230.

Preparation of the adducts

Two adducts were prepared by the reaction of stoichiometric amounts of monoamines (either BA or ODA) and the DGEBA resin MY 790-1 ($n = 0$). Sixty-five grams of DGEBA resin was dissolved in 100 mL of tetrahydrofuran (THF) in a 250-mL glass flask equipped with a reflux condenser to prevent the evaporation of THF. Agitation was achieved with a magnetic stirrer. The flask was placed in an oil bath at 60°C, and the monoamine (BA or ODA) was added dropwise. The mixture was stirred for 3 h at 60°C and then stripped in vacuo at 70°C with a Laborota 4001WB (Heidolph, Schwabach, Germany) for the removal of THF. The adduct obtained with ODA (ADODA) was a wax, whereas the one synthesized with BA (ADBA) was a viscous, transparent liquid at room temperature.

Intercalation of the surface modifiers

Surface modifiers were all exchanged with Somasif ME-100 in the same way, except for the adduct ADBA. First, 120 mequiv of the monoamine, diamine, or triamine per 100 g of Somasif ME-100 was dispersed in deionized water at 80°C. Then, a given quantity of hydrochloric acid (37%) was added to protonate one amine function per surface modifier molecule. Somasif ME-100 was added to the mixture, and a white precipitate formed. It was isolated and washed with deionized water by centrifugation until no chloride was detected in the centrifugate by one drop of a 0.1*N* $AgNO_3$ solution. The adduct ADBA was exchanged in a similar way, except that the adduct was dissolved in a THF/deionized water mixture (8:92). The organosilicates obtained from the cation exchange were dried 2 days at 80°C and then ground in a mill to produce a powder with an average particle size around 80 μm.

Preparation of the epoxy-layered silicate nanocomposites

A given amount of DGEBA resin was heated to 75°C in vacuo with a Labmax high-shear mixer (Molteni AG, Rheinfelden, Switzerland). Then, a quantity of organosilicate corresponding to 5, 10, or 15 wt % of the epoxy system (DGEBA and Jeffamine D230) was added to the DGEBA resin, and the mixture was stirred for 24 h at 75°C to swell the organosilicate in the DGEBA resin. A stoichiometric amount of the curing agent Jeffamine D230 was added. This mixture was stirred in vacuo for 5 min at 75°C and then poured into an aluminum mold previously preheated at 75°C. It was cured for 3 h at 75°C and postcured for 12 h at 110°C. The heating and cooling rates during the curing cycle were 1°C/min. So that the stoichiometry was maintained in all the mixtures, a smaller amount of the curing agent (with the reactive amino groups present in the surface modifiers taken into account) was added when diamine- or triamine-exchanged Somasif ME-100 was used.

IR and NMR

Fourier transform infrared (FTIR) spectroscopy was carried out with a Bruker IFS 88 (Ettlingen, Germany) equipped with a Golden Gate single-reflection atten-

uated total reflectance unit. Each spectrum was the average of 20 scans. ^{1}H-NMR (300 MHz) was achieved with an ARX300 from Bruker.

Both tests were performed on the two adducts (ADBA and ADODA) and their reagents: the DGEBA resin MY 790-1 ($n = 0$), BA, and ODA.

Thermogravimetric analysis

Thermogravimetric analyses were performed with an STA 409 from Netzsch (Selb, Germany). Thirty milligrams of each sample was placed in a crucible and heated at 10°C/min along with a reference under a nitrogen atmosphere (flow rate = 250 cm^3/min). All samples were analyzed from 30 to 700°C. It was assumed that no organic species remained after the thermal analysis.

WAXS

Powder WAXS analyses were performed with a computer-controlled Siemens (Munich, Germany) D500 diffractometer with Cu radiation (50 kV, 40 mA). The scanning speed and the step size were 0.05°/5 s and 0.05°, respectively. The organosilicates were analyzed as produced, whereas the nanocomposites were ground into a powder before their WAXS analysis.

TEM

TEM samples were cut under ambient conditions from nanocomposite blocks with a Reichert & Jung (Vienna, Austria) Ultracut E ultramicrotome equipped with a diamond knife. Thin specimens of about 40 nm were cut from a mesa of about 0.5 × 0.5 mm^2. They were collected in a trough filled with water and placed on 400-mesh copper grids. Transmission electron micrographs were taken with an LEO 912 (Oberkochen, Germany) apparatus at an acceleration voltage of 120 kV. The spacing between neighboring silicate layers was measured manually with ESI-Vision (SIS) analysis software, with the images taken at a magnification of 250,000×. For valid results, the mean value of about 200 measurements was calculated.

Dynamic mechanical thermal analysis

The dynamic mechanical properties of the epoxy resin and filled composites were determined with an RSA II dynamic mechanical analyzer from Rheometrics (dual-cantilever beam test) (Munich, Germany). The measurements covered temperatures from 30 to 140°C at a heating rate of 2°C/min, at a frequency of 1 Hz, and at a 0.05% strain. The sample size was 4 × 2.5 × 50 mm^3. The storage modulus (E'), loss modulus (E''), and damping factor tan δ (E''/E') were derived from each experiment.

Tensile and fracture tests

Young's moduli, tensile strengths, and elongations at break were measured with tensile tests according to ISO 527/95 with a Zwick 1474 machine (Ulm, Germany).

The fracture toughness (K_{IC}) was measured by bend notch tests with a Zwick Flexing 1435 tester according to ISO/DIS 1358. The fracture energy (G_{IC}) was computed from $G_{IC} = (K_{IC}^2/E)(1 - \nu^2)$ because fracture tests were performed under plane strain conditions. E is Young's modulus and ν is Poisson's ratio of the material ($\nu = 0.4$).

The true silicate content, the content of silicate in the composites without surface modifiers, was determined by the weighing of the samples before and after ignition at 1000°C for 2 h. The conversion from a weight percentage to a volume percentage was based on the densities of the polymer and the layered silicate, 1.1 and 2.74 g/cm^3, respectively. The true silicate content was used because surface modifiers contribute to the weight of the organosilicate. The error made in the determination of the true silicate content (wt %) by pyrolysis was about 1%. It was related to water molecules present between the layers and to the removal of OH groups in the layered silicate structure.

In both tests, at least five samples of each composition were tested.

RESULTS AND DISCUSSION

Adduct synthesis

In agreement with an earlier observation by Pinnavaia et al.,[12] the diffusion of DGEBA and curing agent molecules between the silicate layers is a prerequisite for achieving their separation. The role of the surface modifier is to reduce the surface energy of the layered silicate to reduce the electrostatic interactions between the silicate layers and, therefore, favor this diffusion. Pinnavaia et al. showed that long-chain alkylammonium cations such as octadecylammonium cations were good candidates for inducing the formation of epoxy–clay nanocomposites. However, because of the nonpolar nature of their alkyl chain, octadecylammonium cations offer relatively poor compatibility with the epoxy matrix.

Therefore, an adduct was prepared by the reaction of the DGEBA resin with a stoichiometric ratio of ODA. The protonated adduct (ADODA^{2+}) was used in an interlayer gallery cation exchange. The presence of a DGEBA molecule between two alkylamines is expected to afford better compatibility of the surface modifier with the epoxy matrix and, consequently, to improve separation of the silicate layers. Figure 1 denotes the chemical reactions. First, a 2:1 molar ratio of ODA was added to the DGEBA resin MY 790-1 ($n = 0$) in solution in THF and mixed for 3 h at 60°C to

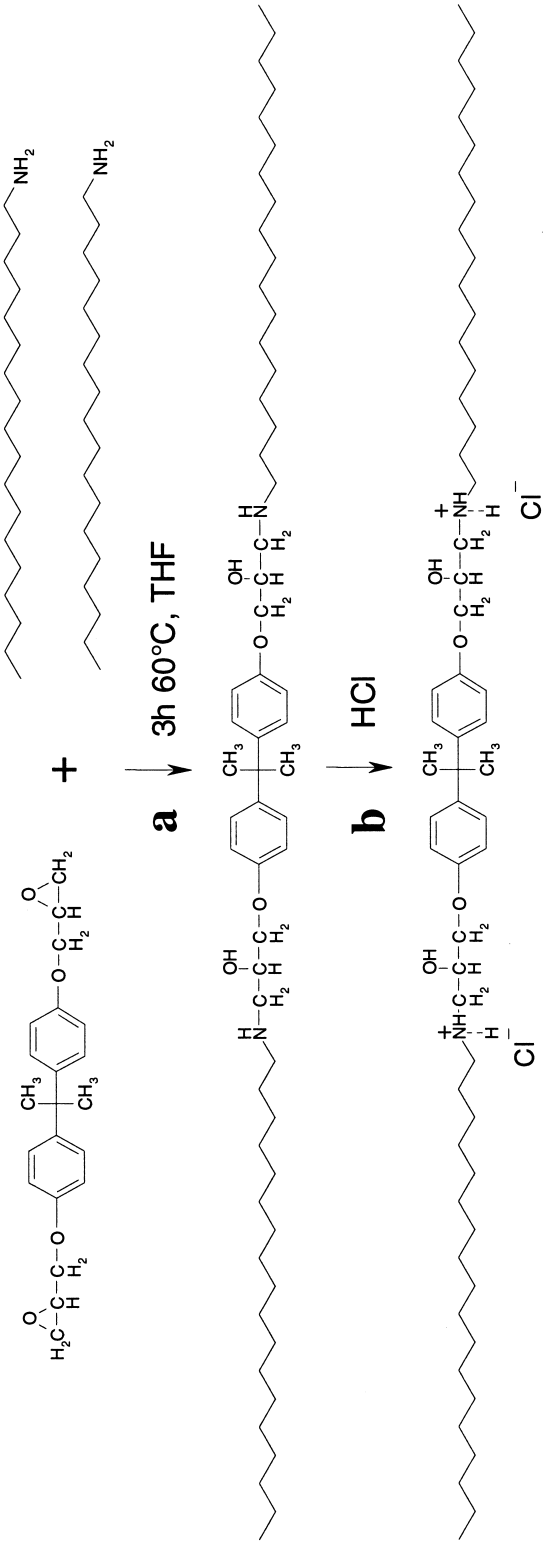

Figure 1 Synthesis of the protonated adduct $ADODA^{2+}$. (a) The first chemical equation represents the reaction of a low molecular weight DGEBA resin ($n = 0$) with two molecules of ODA. (b) The second one shows how the adduct is protonated. Similar reactions were involved in the synthesis of the protonated adduct based on BA ($ADBA^{2+}$).

synthesize the adduct. Then, this adduct was dispersed in a solution composed of deionized water and hydrochloric acid for 3 h at 80°C to protonate the two secondary amine functions. After the addition of the fluorohectorite Somasif ME-100, a white precipitate formed. It was isolated and washed for the removal of the excess residual surface modifier.

Chemical analyses by FTIR and NMR were performed on the new adducts and their reagents to verify that the synthesis was completed. Both analyses confirmed that all epoxy groups of the DGEBA resin had reacted with the ODA molecules.

In the FTIR spectra, absorbency bands corresponding to the stretching of the epoxy rings at 773, 858, and 910 cm^{-1} were clearly visible with the DGEBA but were no longer detectable in the analysis of the adduct ADODA. Moreover, an absorbency band corresponding to the appearance of hydroxyl groups between 3200 and 3600 cm^{-1} was clearly visible in the IR spectrum of the adduct ADODA. This illustrates the fact that as the reaction took place, the epoxy groups opened so that no more stretching of the epoxy rings could be seen and OH groups were progressively formed.

In the NMR spectra, it is the change in the chemical shift of the methine group in the epoxy ring that can be seen after the reaction. This chemical shift of 3.3 ppm in the DGEBA resin is displaced to about 4 ppm in the adduct spectrum. The formation of OH groups in the α position of methine groups during the reaction is responsible for this shift. Because the entire peak is shifted, it illustrates again that all the epoxy groups reacted and confirms the FTIR results. Therefore, we can be confident that the structure of the synthesized adduct ADODA is the one described in Figure 1.

The analyses of the second adduct, ADBA, based on the reaction between a low molecular weight DGEBA resin and BA and synthesized with the same method, gave similar results.

Silicate surface modification

Various organosilicates were obtained via interlayer cation exchange of fluorohectorite (ME-100) with different amines. Table I shows the results of the thermogravimetric analyses performed on the different synthesized organosilicates. Thermogravimetry was used previously to measure the quantity of organic cations exchanged between the silicate layers,[14] and according to one of our recent studies,[15] the determination of the CEC of a layered silicate exchanged with ODA by pyrolysis gave a reasonable value; these measurements were confirmed by the chemical analysis of the layered silicate by inductively coupled plasma atomic emission spectroscopy. Therefore, according to our thermogravimetric analyses of ME–ODA and ME–

TABLE I
Organic Content of the Different Organosilicates

	Quantity of organic cation exchanged (mequiv/100g)	Molecular weight of the surface modifier (g/mol)	Organic content (wt %)
ME–ODA	99	269	27
ME–ADODA	53	879	46
ME–BA	106	107	11
ME–ADBA	50	555	28
ME–JEF M600	56	640	36
ME–JEF D230	55	225	12
ME–JEF D400	50	399	20
ME–JEF T403	36	439	16

BA, the CEC of Somasif ME-100 was about 100 mequiv/100 g. The error made in the determination of the CEC by this method was estimated to be about ±5%.

In the synthesis of organosilicates based on the two adducts (ADODA and ADBA) and the Jeffamines (M600, D230, D400, and T403), protonation of exclusively one amino group in each monoamine, diamine, or triamine molecule was attempted by the addition of a suitable amount of hydrochloric acid to the solution. The idea was to keep unprotonated amino reactive groups, which could then possibly react with the epoxy network during the nanocomposite synthesis. However, according to Table I, the quantity of organic cations exchanged was directly proportional to the number of amino groups in each molecule, except when Jeffamine $M600^{(+)}$ was used. The molar quantity of protonated diamine molecules such as $ADODA^{2+}$ and $ADBA^{2+}$ and also Jeffamines $D230^{(2+)}$ and $D400^{(2+)}$ intercalated between the silicate layers was only half (~50 mequiv/100 g) with respect to that of protonated monoamines such as ODA^{+} and BA^{+} (~100 mequiv/100 g). When the protonated triamine Jeffamine $T403^{(3+)}$ was used, this quantity was only one-third (~36 mequiv/100 g). This indicates that all the amino groups of the intercalated organic ions were protonated even if the amount of hydrochloric acid had been adjusted for the cation exchange. Two hypotheses could account for these results. When the surface modifier is mixed in a water solution with hydrochloric acid, protonation takes place. In the case of triamines, one, two, or three amines are protonated. Most likely, cation exchange of the fully protonated amines can occur much faster. Another hypothesis is that unprotonated amino groups present between the layers experience protonation due to the acidity of the layered silicate. Lagaly[16] reported that the protonation of alkylamines could take place in the presence of clay dispersed in water without the addition of hydrochloric acid. This phenomenon occurs when the surface OH groups are acidic enough that protons can be transferred to the amine group. The fact that the molar quantity of Jeffamine $M600^{(+)}$ intercalated between the silicate layers (56 mequiv/100 g) is much lower than the CEC of the layered silicate (100 mequiv/g) is surprising and may be related to miscibility problems during the cation exchange process.

The second part of Table I shows that the surface modifiers have large differences in their molecular weights. This implies that the organic contents in the different organosilicates are also very different. Therefore, the true silicate content, which is the content of the silicate in the composites without surface modifiers, was used to compare the mechanical properties of the composites synthesized with these different organosilicates.

In Table II, the basal spacings of Somasif ME-100 and all the organosilicates, determined by WAXS, are presented. Their basal spacings were also evaluated by WAXS and TEM after they were dispersed in the epoxy matrix. The reason that Somasif ME-100 presents two basal spacings is easy to understand. The smaller one (9.4 Å) corresponds to the interlamellar spacing of nonhydrated layered silicate, whereas the larger one (12 Å) corresponds to the hydrated form of the layered silicate. In the second case, a monolayer of water molecules is present between the silicate layers. This inhomogeneity in the state of hydration of the layered silicate was not a problem because all the cation exchanges used to synthesize organosilicates took place in water. If we now have a look at the basal spacings of the organosilicates, we can see that they were systematically higher than that of pure Somasif ME-100. This means that all the organic cations were successfully intercalated between the silicate layers during the cation exchange.

However, if we compare the basal spacings of the organosilicates ME–ODA and ME–BA with the ones prepared with their corresponding adducts, namely, ME–ADODA and ME–ADBA, we can see a large difference only between the basal spacings of ME–ODA (19 Å) and ME–ADODA (33 Å). This large difference could be attributed to strong molecular interactions between the nonpolar ODA arms of the adduct and its polar DGEBA body (see Fig. 1). An-

TABLE II
Basal Spacing of the Different Organosilicates Determined by WAXS and TEM Before and After Dispersion in the Epoxy Matrix

	Interlamellar spacing of the organosilicate (Å)	Interlamellar spacing of the organosilicate (5 wt %) in the epoxy matrix (Å)	
	WAXS	WAXS	TEM
ME-100	9.4 and 12	n.d.	n.d.
ME–ODA	19	n.p.	53
ME–ADODA	33	n.p.	58
ME–BA	14	15	14
ME–ADBA	15	15 (broad)	22
ME–JEF M600	17	17	18
ME–JEF D230	13	13	13
ME–JEF D400	17	16	15
ME–JEF T403	14	14	13

n.d. = not determined; n.p. = no peak.

other possibility is that an increase in the *n*-allyl chain length promoted a larger interlamellar distance.

Nanocomposite synthesis

Epoxy-layered silicate nanocomposites were prepared first by the swelling of the organosilicates in DGEBA for 24 h at 75°C. Then, the curing agent was added to the mixture. It was mixed for 5 min in vacuo at 75°C, poured into a preheated mold, cured for 3 h at 75°C, and postcured for 12 h at 110°C. The second column of Table II presents the basal spacings evaluated by WAXS of the different organosilicates incorporated into the epoxy matrix. If we compare these values to the basal spacings of the pure organosilicates presented in the first column, we can see that only the basal spacings of ME–ODA and ME–ADODA were significantly affected by the polymerization of the epoxy. This indicates, according to our WAXS analyses, that the silicate layers were only significantly separated in the nanocomposites based on ME–ODA and ME–ADODA, whereas the other samples were equivalent to conventionally filled composites. According to Messersmith and Giannelis,[17] protonated diamines could bridge intergallery spacings, thereby preventing the separation of silicate layers. However, the organosilicates did not even swell in the DGEBA resin because their interlamellar spacing remained unchanged in the matrix. This suggests that the polarity of the Jeffamines had a negative influence on the diffusion of DGEBA and curing agent molecules between the layers. ME–JEF M600 obtained from fluorohectorite and monoamine-terminated Jeffamine did not promote the separation of the silicate layers, even though no bridging effect was possible with such a surface modifier. However, the fact that ME–JEF M600 was not fully exchanged with Jeffamine M600 may have prevented the diffusion of DGEBA and curing agent molecules into the intergallery spacing. Nevertheless, it appears that effective diffusion is only achieved when octadecyl substituents are introduced to lower the silicate surface energy. A possible explanation for these results is that polar surface modifiers such as Jeffamines do not sufficiently reduce the electrostatic interactions present between the silicate layers to allow the organosilicate to swell in the DGEBA resin.

Finally, the third column of Table II presents the basal spacings evaluated by TEM of different organosilicates incorporated into epoxy. For the conventionally filled composites based on ME–Jeffamines, ME–BA, and ME–ADBA, one can see a very good correlation between the basal spacings determined by WAXS and those measured by TEM. This illustrates the high precision of both methods to evaluate the basal spacings of organized layered silicates and indicates that WAXS and TEM are good complementary methods. However, for the nanocomposites based on ME–ODA and ME–ADODA, the WAXS analysis of which showed no particular order of the silicate layers, we can see that the TEM analyses give additional information about the nanostructures of the layered silicates in the epoxy matrix. TEM reveals that the silicate layers in the two nanocomposites had a long-range order situated around 50–60 Å. The reason that the WAXS analysis did not detect a peak at a low angle corresponding to this basal spacing is because the WAXS method is not suitable for measuring long-range order. If the distribution of basal spacings is large in a nanocomposite, no sharp peak can be seen, and only a poorly visible shoulder can be detected at a low angle. TEM analysis is, therefore, required to characterize correctly the structures of nanocomposites.

Morphology

Figure 2 shows the TEM pictures of two epoxy-layered silicate nanocomposites containing 5 wt % organosilicates modified with ODA and ADODA. As presented

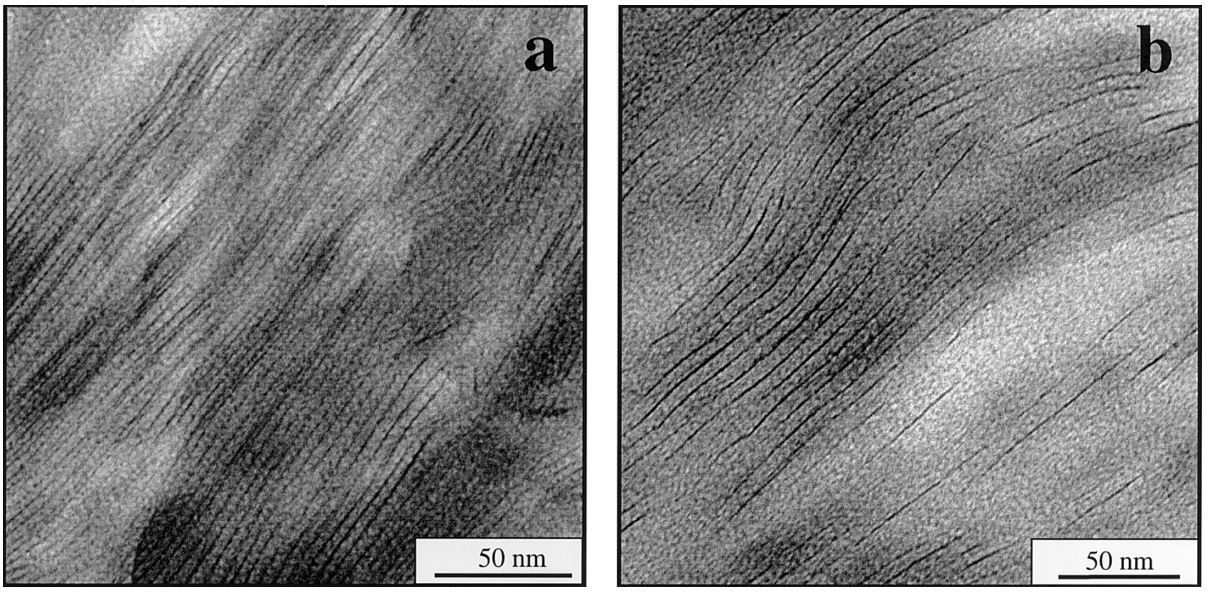

Figure 2 TEM pictures of epoxy-layered silicate nanocomposites containing 5 wt % of the organosilicate modified with (a) ODA and (b) ADODA.

also in Table II, the basal spacing of ME–ADODA in the epoxy matrix (58 Å) is larger than that of ME–ODA (53 Å). According to these results, the presence of the DGEBA molecules in the structure of ADODA promotes the separation of the silicate layers during the polymerization. The polarity of the DGEBA body of the adduct ADODA, as well as hydrogen bridges, probably favors the diffusion of DGEBA and curing agent molecules between the silicate layers, and this improves the separation of the silicate layers upon polymerization. The polarity between the layers may be adjusted by the presence of DGEBA in the molecular structure of the surface modifier so that the separation of the silicate layers is promoted. The use of this adduct illustrates the fact that it is possible to find surface modifiers that are particularly suitable for a given polymer system.

Figure 3 presents the morphologies of composites containing fluorohectorite (Somasif ME-100) exchanged with Jeffamine D400 and the adduct ADODA on a microscale and on a nanoscale. The microstructures of these materials were very similar [Fig. 3(a_1,b_1)]. However, their nanostructure were very different [Fig. 3(a_2,b_2)]. On a microscale, both materials presented aggregates of irregular shapes. On a nanoscale, the nanocomposite synthesized with ME–ADODA contained individual layers separated by a large amount of the polymer, whereas the conventionally filled composite synthesized with ME–JEF D400 presented highly ordered silicate layers with an interlamellar distance of 15 Å. In most of the literature published on this subject, the characterization of these new materials was only performed on a nanoscale, and this could lead to the conclusion that epoxy-layered silicate nanocomposites had a monolithic structure (e.g., a homogeneous nanostructure throughout the material). Figure 3 shows that this is obviously not the case. In fact, here the epoxy-layered silicate nanocomposites were composed of microscale domains of silicate layers separated by more than 50 Å. This illustrates that the characterization of epoxy-layered silicate nanocomposites requires a full description of the material on a microscale. This is especially important for the future modeling of these materials.

Dynamic mechanical properties

Figure 4 shows the evolution of the glass-transition temperature (T_g) of the different composites with their true silicate content. The continuous line indicates T_g of the pure epoxy. The composites synthesized with ME–JEF T403 and ME–JEF M600 are the only materials whose T_g is significantly affected by the presence of the layered silicates. The decrease in T_g with the true silicate content observed for the composite synthesized with ME–JEF T403 (discontinuous line in Fig. 4) is easy to explain. For the stoichiometry to be maintained in all the mixtures, a smaller amount of the curing agent (with the reactive amino groups present in the surface modifiers taken into account) was added when diamine- or triamine-exchanged Somasif ME-100 was used. However, we observed that organosilicates did not exfoliate in the epoxy, so not all amine functions could react with the network. The stoichiometry was no longer respected, so the composite synthesized with the protonated triamine-exchanged organosilicate, ME–T403, presented a steady decrease in its T_g with the true silicate content. The smaller

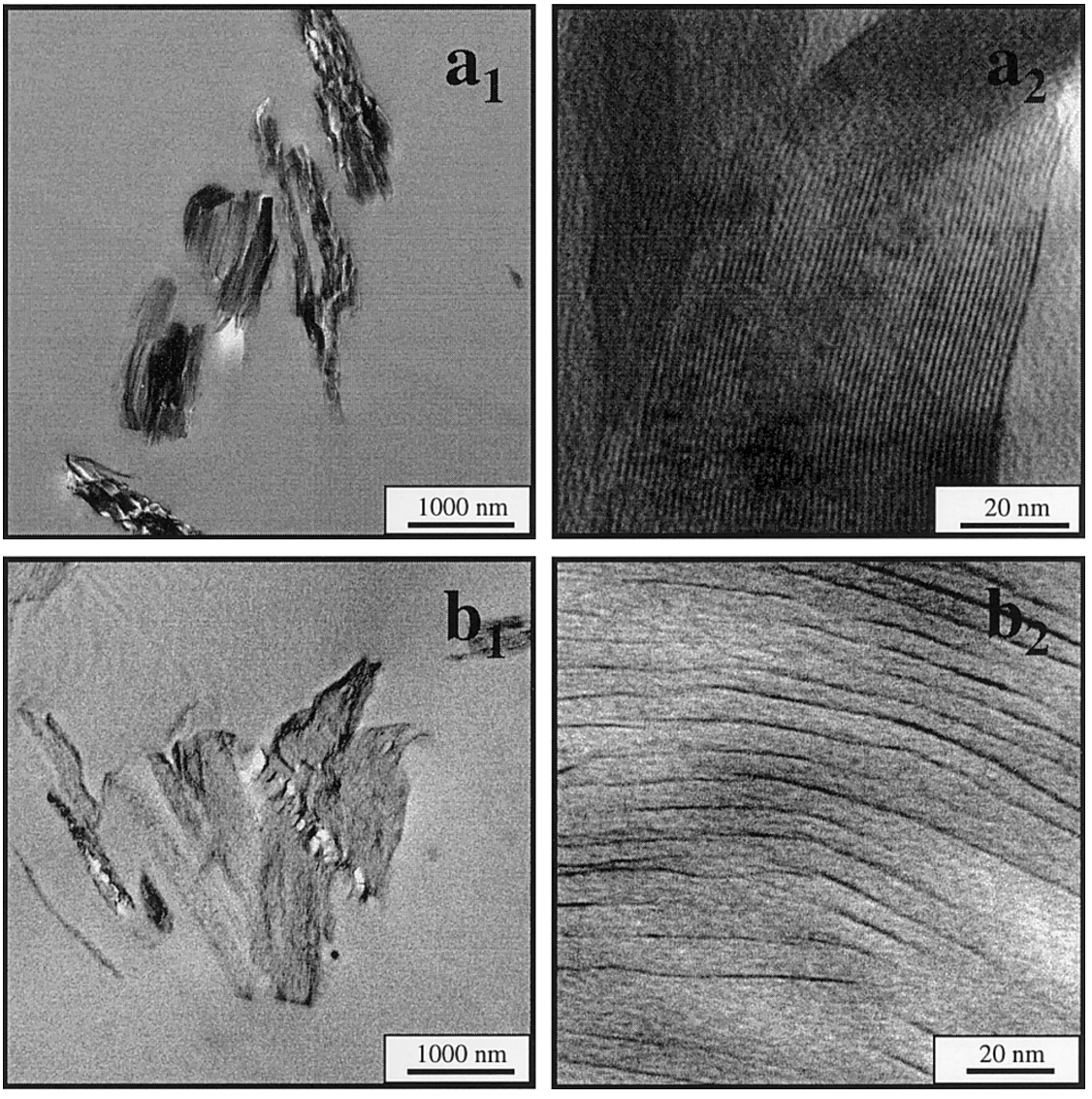

Figure 3 Morphology of the composites synthesized with Somasif ME-100 exchanged with (a_1,a_2) Jeffamine D400 and (b_1,b_2) the adduct ADODA on a microscale and on a nanoscale. The organosilicate content was 5 wt %. (b_1,b_2) These pictures show the presence of microscale domains of silicate layers separated by more than 50 Å for the epoxy-layered silicate nanocomposite.

decrease in T_g observed with ME–JEF M600 could be explained by the possibility of cation exchange during the synthesis. Indeed, because of the high compatibility of ME–JEF M600 with the DGEBA resin, it is possible that when the diamine curing agent was added, it diffused in the neighborhood of the silicate layers, was protonated, and was exchanged with a molecule of Jeffamine M600. This would cause a displacement of stoichiometry, which could explain the decrease in T_g. However, this explanation should be validated by a specific study.

The intensities of the tan δ peaks of the different composites were also compared. This analysis reveals that, at high silicate contents, the intensities of the tan δ peaks corresponding to the nanocomposites synthesized with ME–ODA and ME–ADODA were substantially lower than those for the other composites. This suggests, as

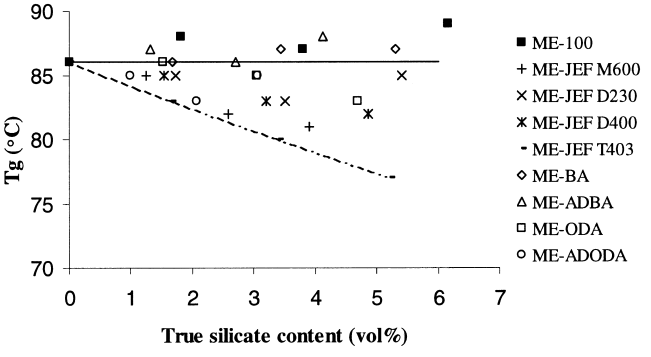

Figure 4 Evolution of T_g with the true silicate content of the different composites. The horizontal continuous line and the discontinuous line indicate T_g of the pure epoxy and the evolution of T_g, respectively, with the true silicate content of the composites synthesized with ME–JEF T403.

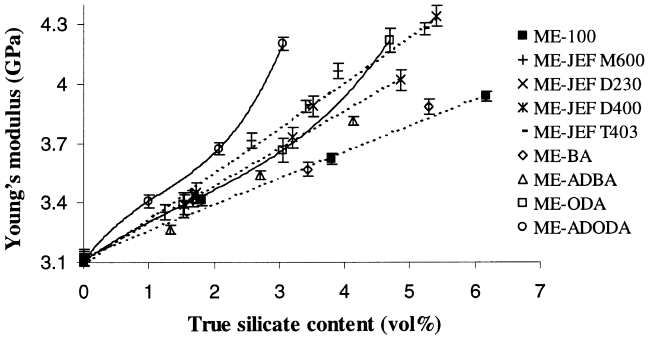

Figure 5 Evolution of Young's modulus with the true silicate content of the different composites. The moduli of the exfoliated nanocomposites synthesized with ME–ODA and ME–ADODA increase parabolically with the true silicate content (continuous curves), whereas those synthesized with ME–JEF D230 and ME–JEF D400 increase linearly (discontinuous lines).

shown in one of our previous articles,[18] a restriction of molecular mobility of the epoxy in the surroundings of the separated silicate layers that was responsible for the decrease in the intensity of the tan δ peaks.

Tensile properties

Figure 5 presents the evolution of Young's modulus with the true silicate content for the different composites. Most of the conventionally filled composites, such as those synthesized with ME–JEF D230 and ME–JEF D400, showed a linear increase in Young's modulus with the true silicate content (see the discontinuous lines in Fig. 5). However, the two nanocomposites synthesized with ME–ODA and ME–ADODA presented a parabolic evolution of Young's modulus with their true silicate content (see the continuous curves in Fig. 5). This was also observed in a different epoxy system[18] and confirms the fact that the separation of the silicate layers modifies substantially the mechanical behavior of these materials. The modulus increase provided by those nanostructures is not clearly understood but could correspond to an increase in the effective volume fraction of the reinforcement in the nanocomposite. As the interlamellar spacing is increased, the effective particle volume fraction is also increased. The corresponding reduction of particle stiffness is a much weaker effect that increases the volume fraction. The low molecular mobility of the polymer matrix in the neighborhood of the silicate layers may contribute to the weak effect of the intercalated polymer on particle stiffness. Moreover, if we compare the two nanocomposites, we find that the modulus increase with the true silicate content is directly related to the degree of separation of the silicate layers. The nanocomposite based on ME–ADODA with an interlamellar spacing of 58 Å shows a steeper increase in modulus with the true silicate content than the nanocomposite based on ME–ODA, for which the interlamellar spacing is 53 Å. For a true silicate content of 3 vol %, the nanocomposite based on ME–ADODA shows an increase in modulus of 34% with respect to the pure epoxy.

Figure 6 presents the evolution of the tensile strength and elongation at break with the true silicate content of the different composites. It is clear that the nanocomposite based on ME–ADODA presents a different behavior than the other composites. Indeed, the tensile strength remains roughly unchanged as the true silicate content is increased for all the composites, except for the nanocomposite based on ME–ADODA. The fact that the nanocomposite based on ME–ODA does not show a similar trend indicates that the difference observed is not directly related to the material nanostructure. Manufacturing problems could be responsible for this difference. Indeed, problems were encountered when ME–ADODA was reduced into a powder. Because of the large size of the intercalated ions, the particles tended to stick to one another during the powder preparation. This resulted in the presence of a few relatively large microaggregates in the nanocomposite plates because the particles were not completely dispersed during the swelling of the organosilicate in the DGEBA resin. These few aggregates may act as stress concentrators, lowering significantly the tensile strength. This illustrates the influence of the microstructure of the nanocomposites on the mechanical properties. The elongation at break of the different composites decreases linearly with the true clay content (see the discontinuous line in Fig. 6), except for the nanocomposite based on ME–ADODA for the same reason.

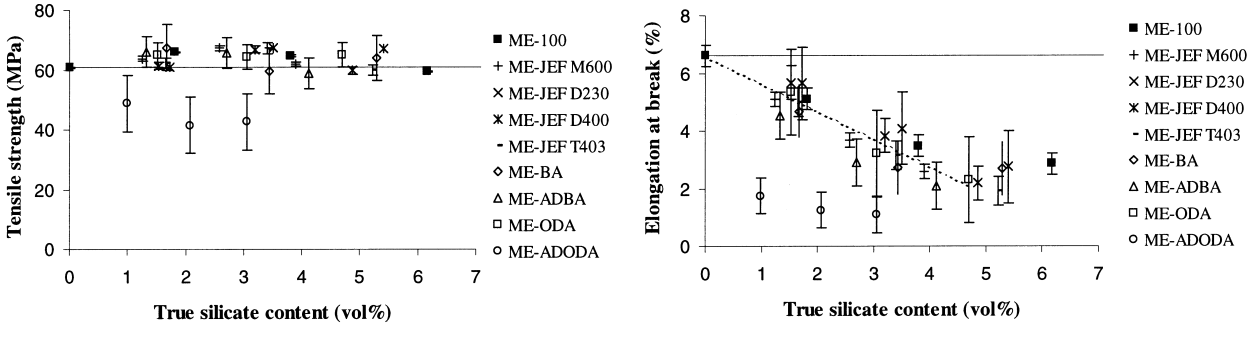

Figure 6 Evolution of the tensile strength and the elongation at break with the true layered silicate content of the different composites. The horizontal lines indicate the strength and elongation at break of the pure epoxy.

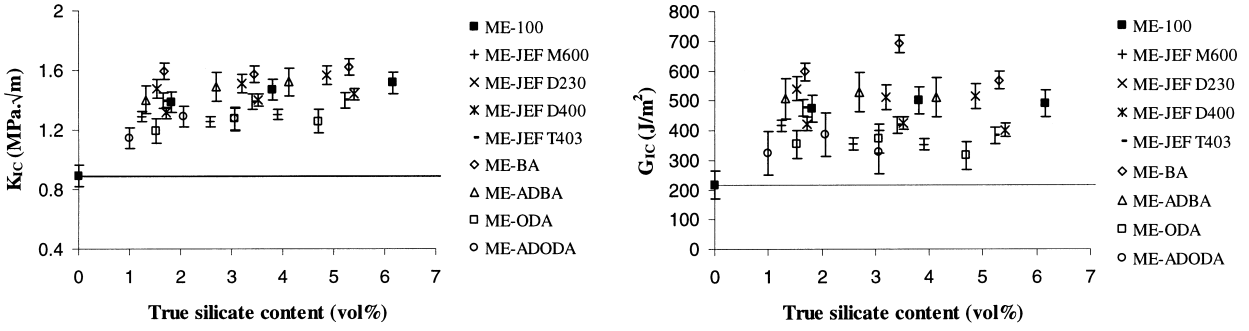

Figure 7 Evolution of K_{IC} and G_{IC} with the true silicate content of the different composites. The horizontal lines indicate K_{IC} and G_{IC} of the pure epoxy.

Fracture properties

Figure 7 presents the evolution of K_{IC} and G_{IC} with the true silicate content for the different composites. All the composites performed better than the pure epoxy. An improved toughness/stiffness/strength balance as a result of silicate surface modification combined with epoxy resin matrix compatibilization was also reported for anhydride-cured epoxy nanocomposites.[19] The two nanocomposites based on ME–ODA and ME–ADODA, which had different degrees of silicate layer separation, showed similar variations, and the best performances were obtained for the conventionally filled composites based on ME–BA.

First, these results indicate that the fracture behavior of nanocomposites is apparently independent of the degree of separation of silicate layers. The lower performance of the nanocomposites with respect to the other conventionally filled composites is possibly related to the size of the microaggregates. In nanocomposites, layered silicates are dispersed in the epoxy matrix as swollen microaggregates with a large interlamellar spacing, whereas in conventionally filled composites, those aggregates are smaller.

CONCLUSIONS

A comparison of the nanostructures of epoxy-layered silicate nanocomposites prepared with fluorohectorite exchanged with ODA or Jeffamines indicates that the polarity of the surface modifier has an important influence on their morphology. This might be due to the fact that polar surface modifiers do not reduce sufficiently the electrostatic interactions present between the silicate layers so that the corresponding organosilicates do not swell in the DGEBA resin.

A microstructural characterization performed by TEM shows that, in this epoxy system, nanocomposites are composed of microscale domains of parallel silicate layers separated by more than 50 Å. Even if these nanocomposites are not truly exfoliated because they still have a long-range order, they present unusual mechanical behavior. Therefore, Young's modulus of the nanocomposites increases parabolically with the true silicate content, whereas the modulus of conventionally filled composites shows a linear increase at a low silicate content. Fracture properties are not substantially affected by the nanoscopic separation of the silicate layers and are mostly improved for conventionally filled composites. This suggests that mechanisms governing fracture properties of these materials are occurring on the microscale.

Diplom-Chem Jörg Fröhlich from the Freiburg Materials Research Centre is acknowledged for fruitful discussions and for his help with the experimental work.

References

1. Yano, K.; Usuki, A.; Okada, A.; Kurauchi, T.; Kamigaito, O. J Polym Sci Part A: Polym Chem 1993, 31, 2493.
2. Lan, T.; Pinnavaia, T. J. Chem Mater 1994, 6, 2216.
3. Messersmith, P. B.; Giannelis, E. P. J Polym Sci Part A: Polym Chem 1995, 33, 1047.
4. Kojima, Y.; Fukumori, K.; Usuki, A.; Okada, A.; Kurauchi, T. J Mater Sci Lett 1993, 12, 889.
5. Massam, J.; Pinnavaia, T. J. Mater Res Soc Symp Proc 1998, 520, 223.
6. Gilman, J. W.; Kashiwagi, T.; Lichtenhan, J. D. SAMPE J 1997, 33, 40.
7. Less, J.; Takekoshi, T.; Giannelis, E. P. Mater Res Soc Symp Proc 1997, 457, 513.
8. Usuki, A.; Kawasumi, M.; Kojima, Y.; Okada, A.; Kurauchi, T.; Kamigaito, O. J Mater Res 1993, 8, 1174.
9. Usuki, A.; Kawasumi, M.; Kojima, Y.; Okada, A.; Kurauchi, T.; Kamigaito, O. J Mater Res 1993, 8, 1179.
10. Jordan, J. W. J Phys Colloid Chem 1949, 53, 294.
11. Weiss, A. Angew Chem Int Ed 1963, 2, 134.
12. Lan, T.; Kaviratna, P. D.; Pinnavaia, T. J. Chem Mater 1995, 7, 2144.
13. Kornmann, X.; Lindberg, H.; Berglund, L. A. Polymer 2001, 42, 1303.
14. Zilg, C.; Mülhaupt, R.; Finter, J. Macromol Chem Phys 1999, 200, 661.
15. Kornmann, X.; Lindberg, H.; Berglund, L. A. Polymer 2001, 42, 4493.
16. Lagaly, G. Solid State Ionics 1986, 22, 43.
17. Messersmith, P. B.; Giannelis, E. P. Chem Mater 1994, 6, 1719.
18. Kornmann, X.; Lindberg, H.; Berglund, L. A. Mater Res Soc Symp Proc 2000, 628, CC11.8.
19. Zilg, C.; Thomann, R.; Finter, J.; Mülhaupt, R. Macromol Mater Eng 2000, 280, 41.